

# A Low-Profile and Beam-tilted Continuous Transverse Stub Array Antenna at W-band

Demiao Chu, Yujun Xiong, and Ping Li

School of Optical-Electrical and Computer Engineering  
University of Shanghai for Science and Technology, Shanghai, 200093, China  
liping@usst.edu.cn

**Abstract** — This paper presents a low-profile, high gain, beam-tilted continuous transverse stub (CTS) array antenna at W-band. The antenna comprises 32 radiating slots and is fed by a parallel plate waveguide (PPW) network with a linear source generator. To deflect the outgoing beam, the principle of linear array scanning is adopted to design inverted T-type structure in each stub to introduce wave path difference. PPW network allows the antenna to obtain lower profile compared to other transmission lines. The design procedure, and the antenna characterization are described. The main beam of the antenna is tilted 12 degree in H-plane. The simulation and measured results show that this antenna achieves peak gain of 32.4 dB and a 12 degree beam tilt angle at 99GHz. S11 parameters of the antenna is less than -10 dB in a broadband from 96 GHz to 103 GHz. This antenna has an advantage of miniaturization over other high-gain antenna solutions. The promising performance of this proposed CTS antenna reveals the possible candidate for Millimeter wave (MMW) telecommunication applications.

**Index Terms** — CTS array antenna, pillbox, W band.

## I. INTRODUCTION

Millimeter wave (MMW) technology is becoming increasingly attractive in the future of telecommunications. Stringent requirements are imposed on the antennas which not only need high gain but also require a tilted beam. We can refer to several solutions to try to satisfy these previous requirements such as classical parabolic systems and electromechanical scanning planar antenna arrays [1]. However, the parabolic systems are bulky, and its size is too big to flexibly move on the platform, while the high requirements manufacturing precision of electromechanical scanning planar antenna arrays leads to high cost [2,3]. Therefore, it is necessary to study a miniaturized, low-cost MMW antenna with high gain and tilted beam.

Due to the attractive performance and manufacturing stability, Continuous Transverse Stub (CTS) array antennas can be considered as good candidates for

advanced antenna systems. The profile of CTS array antennas can be reduced at lower cost and radiation performance could be improved [4]. The CTS array antenna was first proposed in the early 1990s [5-8], which is evolved from the parallel-plate waveguide. In 1998, Chu of EMS Lab used the Floquet mode method [9] to analyze the radiation theory of CTS array antenna and perfect its basic theories. The main structure of a CTS array antenna is a one-dimensional (1-D) array of parallel-plate waveguide with parallel lateral openings. The electromagnetic waves are radiated from the parallel-plate waveguide and the impedance can be optimized by adding series of stubs. Over the past two decades, the CTS array antenna has evolved many types and been applied in various fields, such as True-Time-Delay (TTD) CTS and Multi-channel Video and Data Distribution Service (MVDDS), etc. [10]. Moreover, the increasing number of stubs can enlarge the antenna gain. In such a way, CTS array antennas have the ability to improve performance in high gain and broadband conditions. On the other hand, the increasing demand for satellite telecommunications and radar applications stimulate the increasing development of waveguide-based CTS array antenna, such as coaxial-waveguide type [11,12], coplanar-waveguide type [13,14] and rectangular-waveguide type [15]. However, those CTS antennas in conventional configurations adopt normal radiation. That is, when there needs an azimuth angle-between the antenna's normal direction and the target, a tilted beam that deviates from the normal direction of the antenna plane would be required.

Motivated to design a low-profile and beam-tilted CTS array antenna at W-band, a 32-slot CTS array antenna and 12 degree beam deflection angle working in the frequency band of 96-103 GHz is proposed. The antenna is fed by a pillbox, whose structure has a lower profile compared to the multiplexed power split structure. The impedance transformers in the design are introduced not only for the feeding network, but also for the radiation stubs. This method can optimize the return loss, reduce the size of the entire antenna and improve the antenna efficiency through structure and parameter

optimization. The radiating stubs of 32 slots are adjusted which are based on the principle of linear array scanning to contain an inverted T-type structure for realizing an azimuth-angle inclination. The final thickness of the antenna is 30 mm and can be further reduced by dielectric filled (parallel plate waveguide) PPW feeding network. Measurements of antenna performance are very promising and reveal the possibilities of CTS array offers for MMW communication applications.

## II. ANTENNA DESIGN

Among all antenna structures, CTS array antennas are very different from other types of planar array antennas in the field of radiating realization, coupling mechanism, transmission-line properties, and feeding network [15]. Figure 1 illustrates a typical CTS array antenna structure, realized by a wide and continuous array of short transverse radiating stubs. CTS array antenna is of limited height, extending from the upper conductive plate of an open parallel plate transmission structure, internally excited by a linear source. These stubs interrupt the longitudinal current component within the parallel plate transmission structure and effectively couple and radiate propagating energy from the parallel plate structure into free space as a linearly polarized wave.

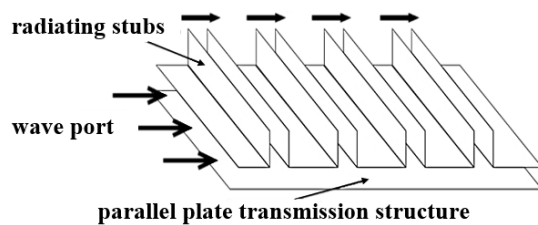


Fig. 1. Typical cross-sectional view of a CTS array.

In order to achieve a low-profile and high-gain CTS array antenna with an angle of beam inclination, the number of radiating stubs required is significant, all parts of the antenna need to be simulated and tolerance analysis according to principle of phased array beam control [16]. As shown in Fig. 2 (a), the CTS array antenna proposed in this paper consists of two main parts: The CTS array (CTS radiation stubs and parallel plate waveguide network) and a linear source generator. The CTS array contains 32 radiating stubs which are connected to the end of the power divider, the pillbox structure effectively reduces the overall height of the antenna by using an embedded two-dimensional (2-D) parabolic reflector. The beam emitted by the CTS array antenna is at a fixed declination to the antenna's normal direction, the application scenario rendering of the CTS antenna proposed in this paper is shown in Fig. 2 (b). Details of the CTS array antenna proposed in this paper are shown in Fig. 2 (a), inverted T-type structure is the

reason for the tilted beam of the antenna. The overall size of the CTS array antenna is 60mm \* 60mm \* 30mm, which mainly comprises the CTS array and the linear source generator.

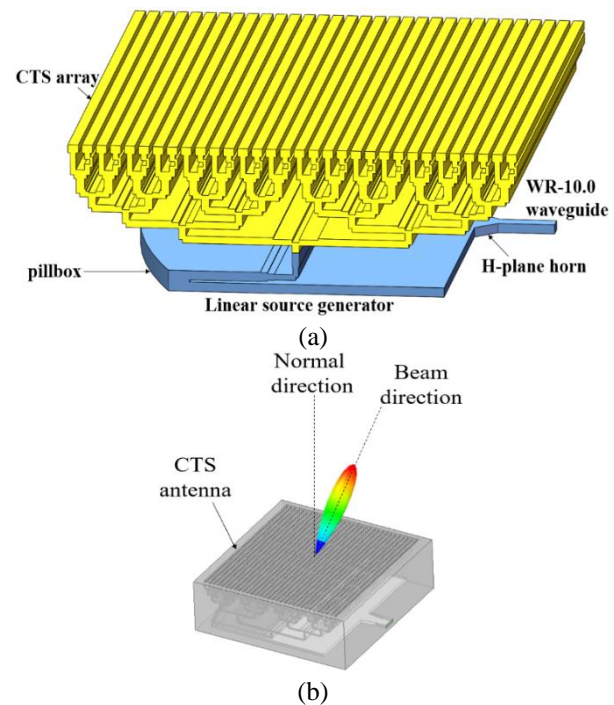


Fig. 2. Perspective view of the CTS array antenna: (a) Front view and (b) application scenario rendering.

### A. The CTS array

As shown in Fig. 3, the CTS radiating stubs which are composed of 32 sections attach to the parallel plate waveguide network. The reflection coefficient of the radiation stubs depends on the width of stub ( $a$ ), the array spacing ( $d$ ) and dielectric constant of filled material within an operational frequency range. In order to achieve a good impedance match for broadband transmission, the radiating stubs are fed with the same amplitude and phase by the parallel plate waveguide network which consists of a parallel 1-to-32 power divider [17].

The beam inclination angle can be achieved by using an inverted T-type structure [18]. In such a way, the inverted T-type structure in this paper has been designed to steer the antenna beam to 12 degree in the azimuth plane. Phased array scanning and positioning are used here. For phase-controlled scanning of the beam in space, each radial array element is connected to a variable phase shifter. Inverted T-structure creates a wave path-difference between adjacent radiating stubs.

In the direction of deviation from the antenna normal to  $\theta$  degree, the phase difference between the two adjacent array elements:

$$\Phi_B = 2\pi d \sin\theta / \lambda, \quad (1)$$

where  $d$  is the width of two adjacent periodic stubs,  $\lambda$  is the wavelength at the center frequency. It is caused by the wave path-difference of the target echo. Due to the nonzero phase difference between the array elements, the antenna normal direction of each array element of the radiation field strength cannot be summed, such that the antenna normal direction is no longer the direction of the largest field strength. In the direction of deviation from the antenna normal to  $\theta$  degree, the maximum value is obtained by adding the field strengths in the same phase, and the beam direction changes from the array normal to the direction of deviation from the antenna normal to  $\theta$  degree. By changing the phase difference  $\Phi_B$  between neighboring cells in the array, we can have a titled beam at  $\theta$ , which can change the direction of the antenna beam. Then, the wave path-difference can be calculated as:

$$d\tau = d\sin\theta. \tag{2}$$

This will give the wave path-difference as needed.

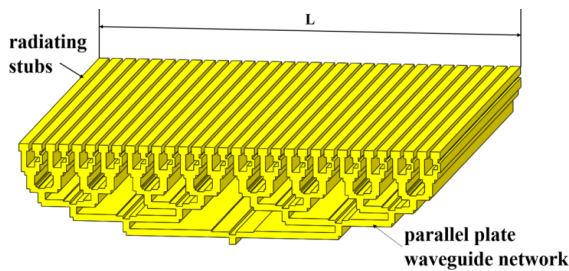


Fig. 3. Perspective view of the CTS array.

As shown in Fig. 4, every node of the parallel plate waveguide network is composed of an E-plane T-section and a multi-stage matching step. A multi-stage matching step based on Chebyshev impedance transformation theory [19] is designed, and the final size is determined in accordance with simulation and optimization.

The final array consists of 32 radiating stubs, and the original array spacing is set as  $\lambda/2$  ( $\lambda$  is the wavelength at the center frequency). The center frequency of the design is 99 GHz (corresponds to a wavelength of 3mm in vacuum). The dimensions of stubs is illustrated in Fig. 5 (a). By setting  $f_c=99$  GHz, the stub width  $a < a_{max} = \lambda/2 = 1.502$ mm. On the other hand, as discussed in [19], for a given width of two adjacent periodic stubs  $d$ , the real part of the active slot impedance  $Z_{act}$  in the H-plane of a CTS array increases when  $a$  decreases. The active slot impedance of an infinite CTS array with this value for  $(d+a)$  has been computed for different slot widths, approaching its upper bound of  $(d+a_{max})$ , by using the numerical model presented in [19]. Each active impedance is normalized with respect to the characteristic impedance  $Z_0 = \eta a/\omega$  of a PPW line having its height equal to the slot width  $a$  and a unitary length  $\omega$ , where  $\eta$  is the free-space impedance. Bringing back to the numerical model presented in [19], calculation results demonstrate that for  $(d+a) = 1.5$  mm, the imaginary part

of the slot active impedance experiences limited variations and in low resistance. Therefore, the stub width  $a$  is set as  $0.66a_{max} = 1$  mm and  $d = 0.5$  mm. According to the mathematical model used to calculate  $d$ , the wavelength difference between two adjacent radiating stubs  $d\tau$  is set to 0.104mm. As shown in Fig. 5 (a), after analysis of the simulation results, the best impedance matching is achieved when the inverted T-type structure is set at 0.76mm from the top of the radiating stubs and the length is 0.64mm. The equivalent circuit diagram of the end of the radiating branch with the inverted T-type structure added is shown in Fig. 5 (b). Phase difference between adjacent radiating stubs at the Y-port due to the difference in signal transmission distance

As shown in Fig. 5 (c), the E-plane T-section is a classical power divider in PPW technology associating to a quarter wavelength transformer, so the input and output ports have the same characteristic impedance and width (0.7 mm). The quarter-wavelength transformer of width 0.5 mm is used to halve the impedance value at the output ports before joining the section with width 0.36 mm.

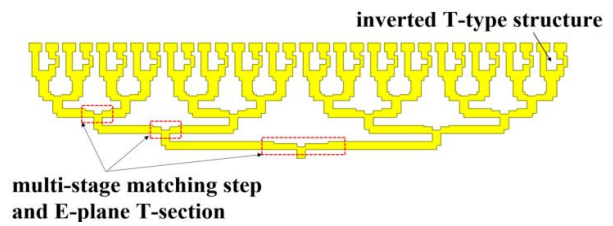


Fig. 4. Cross-section view of the CTS array.

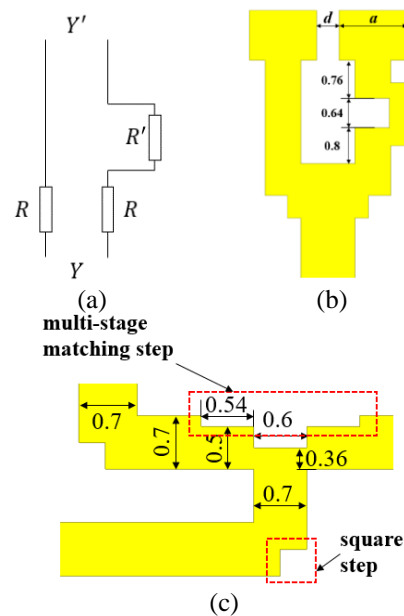


Fig. 5. E-plane cross-sectional view: (a) inverted T-type structure; (b) inverted T-type structure's equivalent circuit; (c) E-plane T-section. All dimensions are given in millimeters.

## B. Linear source generator

The selection of feeding network is crucial. Existing feeding network contains a combination of a power divider and a radiator, pillbox, lens array, etc. [20]. There are two combinations (vertical and horizontal methods) to connect a power divider to a radiator. The horizontal method allows for lower profile compared with the vertical one, but both approaches are difficult to be used in a broadband application for the complexity and bandwidth limitation of the power divider. The attractive characteristics of pillbox are low-cost, compactness and miniaturization [21]. In order to achieve low profile and low cost, a pillbox is used in this paper. In the pillbox, various modes exist between the two plates according to the distance between parallel plates [22]. The pillbox supports free propagation of a principal wave (TEM-mode) in which the electric vector is normal to the plates, and the velocity of propagation and the wavelength are the same as in free space. TE and TM modes are also possible in a pillbox, which correspond to the modes in a rectangular waveguide [23].

As shown in Fig. 6, the linear source generator consists of a pillbox and an H-plane horn. The pillbox generates a linear source to excite the parallel plate waveguide network. The H-plane horn is fed by a standard WR-10.0 waveguide. The horn is located in the focal plane of the 2-D parabolic reflector. The H-plane horn and the pillbox are placed in the parallel plate waveguides and are same in height. Figure 7 shows a top view and a cross-sectional view of the linear source generator. It is made by two stacked PPW lines and a long slot with a width of 2.3 mm coupled through a spherical crown. The 2-D parabolic reflector in the common metal plate is contoured between the two PPW lines with the distance of 0.51 mm. As Fig. 7 (a) shows, the pillbox couplers designed here have the following parameters: the diameter of the pillbox length, denoted as  $D$ , the focal length of the parabola, denoted as  $F$ , the focal horn aperture as shown in Fig. 6. To match the parallel plate waveguide network, the diameter  $D$  is equal to length  $L$  (shown in Fig. 3) of the CTS radiating stubs. Once the parabola diameter has been selected, the focal length  $F$  and the focal horn aperture are to be chosen together [24]. In this work, we set the diameter  $D=19.8\lambda=60\text{mm}$  and the focal length  $F=15.2\lambda=46\text{mm}$  together with a horn width of 10.32 mm. Finally, a 90 degree bend with a stair-step height of 0.46mm connects the pillbox transition to the input port of the corporate-feed network after a three-layer decreasing rectangular waveguide structure. The three-layer decreasing rectangular waveguide structure can filter out high sub-modes in the structure.

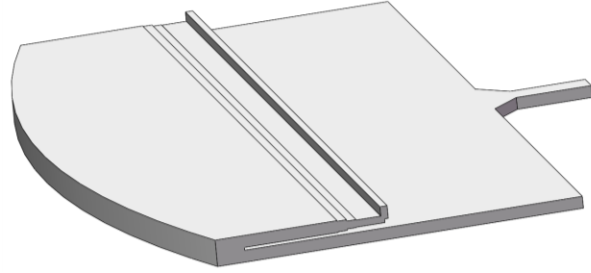


Fig. 6. 3-D view of the linear source generator.

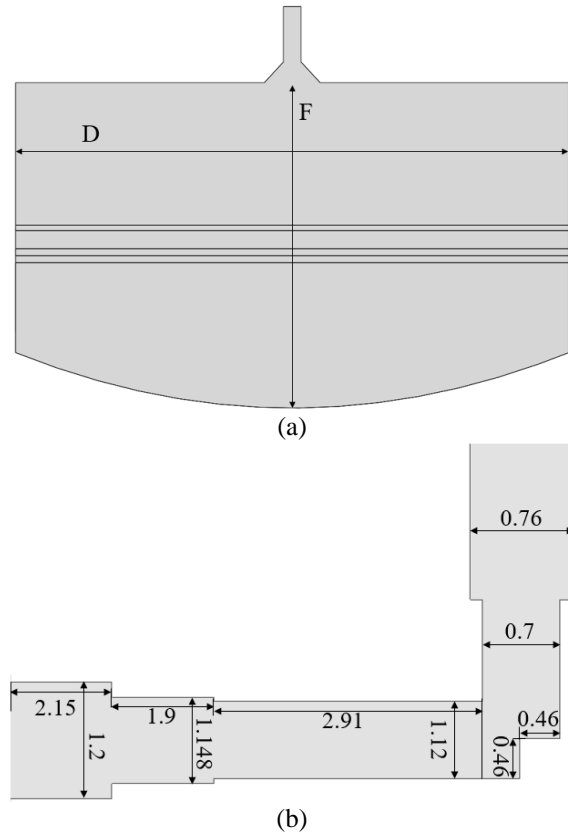


Fig. 7. (a) Top view and (b) cross-sectional view of the linear source generator. All dimensions are given in millimeters.

## III. RESULT

The designed CTS array antenna was simulated by ANSYS Electronics Desktop HFSS 19.0. Based on the parameter optimization of CTS radiation stubs and waveguide feeding network, the results meet the design requirement of antenna.

The antenna in this paper is realized by gold-plated copper. An efficient method based on separate module

fabrication and screw assembly is used to simplify the fabrication process. The standard method of manufacturing hollow the CTS array and the pillbox relies on an expensive joining or brazing process and connecting the pillbox to the CTS array. The processed antenna is shown in the Fig. 8.

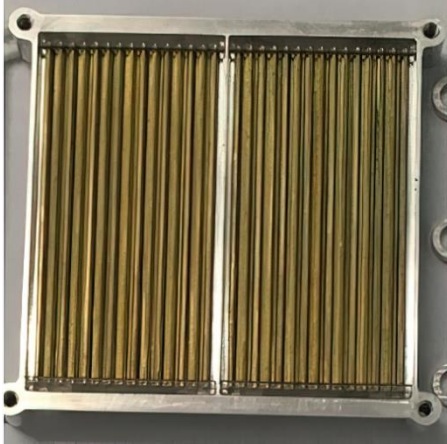


Fig. 8. Top view of antenna prototype.

The S-parameters and directional maps of the processed antenna are measured and also are compared with the simulation results. We use the Agilent N5227A PNA network analyzer and a set of WR-10 (75–110 GHz) VNA extenders to characterize the device transmission and using the method of rotating the antenna to test antenna pattern. The good agreement between the simulation and measurement is shown as following. Figure 9 (a) shows the simulation and measured results of the antenna reflection coefficient. The operating frequency band is 96 GHz to 103 GHz (relative working bandwidth: 7%), and the reflection coefficient is less than -10 dB in available frequency band. Fig. 9 (b) shows the simulation and measured results of the gain in E-plane at 99 GHz. The pattern shows that the gain is 32.5 dB at 99 GHz and normalized side lobe level is less than -12dB. The azimuth of the beam is 12 degree and the HPBW is 2.56 degree. We can see from the measured result that there is a peak gain of 31.6 dB at the center frequency of 99 GHz, the normalized side lobe level is less than -12dB. The gain of this antenna is over than 30 dB in the frequency range of 96-103 GHz. The beam has a deflection angle of approximately 12 degree. HPBW of this antenna is about 2.4degree. The measured peak gain is slightly lower than that in the simulation. The small difference may be attributed by the assembly error and the fabrication tolerance.

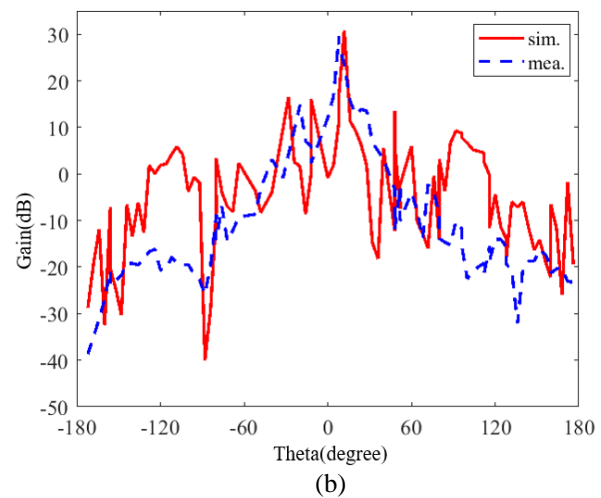
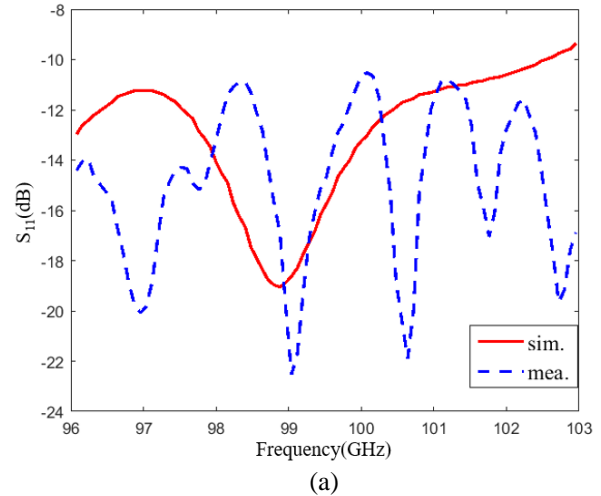


Fig. 9. (a) Simulated and measured  $S_{11}$  parameters of the CTS antenna. (b) Simulated and measured radiation patterns at the frequency of 99 GHz.

#### IV. CONCLUSION

This paper presents a CTS array antenna with low profile, high gain, high efficiency and 12 degree beam deflection angle. This antenna consists of CTS array (CTS radiation stubs and parallel plate waveguide network) and a linear source generator, which can be independently designed and optimized. We change the radiating stubs by the inverted T-type structure to realize an azimuth angle of inclination. This CTS antenna utilizes multistage impedance converter to increase radiation efficiency and achieve a higher gain and lower side lobe in feeding network and radiation components compared with other CTS antennas. And the pillbox structure of the linear source generator is also used to

implement this low-profile CTS array antennas. It has been demonstrated that the structure can be an attractive candidate for the through-the-wall detection system based on terahertz technology.

### ACKNOWLEDGMENT

This work was supported in part by the National Key R&D Program of China (2018YFF01013003), in part by the National Natural Science Foundation of China (61731020, 61722111).

### REFERENCES

- [1] Y. Asci, E. Curuk, K. Yegin, and C. Ozdemir, "Improved splash-plate feed parabolic reflector antenna for Ka-band VSAT applications," *2016 46th European Microwave Conference (EuMC)*, London, pp. 1283-1286, 2016.
- [2] M. Tripodi, F. Dimarca, T. Cadili, C. Mollura, F. Dimaggio, and M. Russo, "Ka-band active phased array antenna system for satellite communication on the move terminal," *2012 IEEE First AESS European Conference on Satellite Telecommunications (ESTEL)*, Rome, pp. 1-4, 2012.
- [3] M. Shelley, J. Vazquez, and D. Moore, "X- and Ka-band low profile antennas for aeronautical and land mobile satcom," *The 8th European Conference on Antennas and Propagation (EuCAP 2014)*, New York, pp. 2619-2622, 2014.
- [4] W. W. Milroy, "Continuous transverse stub element devices and methods of making same," U.S. Patent No. 5,266,961, Nov. 30, 1993.
- [5] W. W. Milroy, "Antenna array configurations employing continuous transverse stub elements," U.S. Patent No. 5,349,363, Sep. 20, 1994.
- [6] W. W. Milroy, "Continuous transverse stub element device antenna array configurations," U.S. Patent No. 5,412,394, May 2, 1995.
- [7] W. W. Milroy, "Continuous transverse stub element devices for flat plate antenna arrays," U.S. Patent No. 5,483,248, Jan. 9, 1996.
- [8] W. W. Milroy, "Radar and electronic warfare systems employing continuous transverse stub array antennas," U.S. Patent No. 5,469,165, Nov. 21, 1995.
- [9] R.-S. Chu, "Analysis of continuous transverse stub (CTS) array by floquet mode method," *IEEE Antennas and Propagation Society International Symposium*, Atlanta, pp. 1012-1015, 1998.
- [10] W. H. Henderson and W. W. Milroy, "Wireless communication applications of the continuous transverse stub (CTS) array at microwave and millimeter wave frequencies," *IEEE/ACES International Conference on Wireless Communications and Applied Computational Electromagnetics*, Holonunu, pp. 253-256, 2005.
- [11] M. F. Iskander, Z. Zhang, Z. Yun, and R. Isom, "Coaxial continuous transverse stub (CTS) array," *IEEE Microwave and Wireless Components Letters*, vol. 11, no. 12, pp. 489-491, Dec. 2001.
- [12] J. Qiu, X. Xing, and L. Zhong, "A novel coaxial CTS antenna design," *2007 6th International Conference on Antenna Theory and Techniques*, Sevastopol, pp. 323-325, 2007.
- [13] W. Kim and M. F. Iskander, "A new coplanar waveguide continuous transverse stub (CPW-CTS) antenna for wireless communications," *IEEE Antennas and Wireless Propagation Letters*, vol. 4, pp. 172-174, 2005.
- [14] L. Yue, M. F. Iskander, Z. Zhang, and Z. Feng, "A phased CPW-CTS array with reconfigurable NRI phase shifter for beam steering application," *2013 IEEE International Wireless Symposium (IWS)*, Beijing, pp. 1-3, 2013.
- [15] X. Pan, F. Yang, S. Xu, and M. Li, "W-band electronic focus-scanning by a reconfigurable transmitarray for millimeter-wave imaging applications," *Applied Computational Electromagnetics Society Journal*, vol. 35, no. 5, pp. 580-586, May 2020.
- [16] N. Seman, K. H. Yusof, and M. H. Jamaluddin, "Ultra-wideband six-port network constructed by 90° and in-phase power dividers," *Applied Computational Electromagnetics Society Journal*, vol. 34, no. 5, pp. 689-695, May 2019.
- [17] S. X. Ta, C. D. Bui, and T. K. Nguyen, "Wideband Quasi-Yagi antenna with broad-beam dual-polarized radiation for indoor access points," *Applied Computational Electromagnetics Society Journal*, vol. 34, no. 5, pp. 654-660, May 2019.
- [18] T. Potelon, M. Ettorre, L. L. Coq, T. Bateman, J. Francey, D. Lelaidier, E. Seguenot, F. Devillers, and R. Sauleau, "A low-profile broadband 32-slot continuous transverse stub array for backhaul applications in E-Band," *IEEE Transactions on Antennas and Propagation*, vol. 65, no. 12, pp. 6307-6316, Dec. 2017.
- [19] F. F. Manzillo, M. Ettorre, M. Casaletti, N. Capet, and R. Sauleau, "Active impedance of infinite parallel-fed continuous transverse stub arrays," *IEEE Trans. Antennas Propag.*, vol. 63, no. 7, pp. 3291-3297, July 2015.
- [20] P. Zhang, R. Mittra, and S. Gong, "Compact line source generator for low profile continuous transverse stub array antenna," *2016 International Workshop on Antenna Technology (iWAT)*, Cocoa Beach, pp. 77-79, 2016.
- [21] K. Tekkouk, M. Ettorre, E. Gandini, and R. Sauleau, "Multibeam pillbox antenna with low sidelobe level and high-beam crossover in SIW technology using the split aperture decoupling method," *IEEE Transactions on Antennas & Propagation*, vol. 63, no. 11, pp. 5209-5215, Nov.

- 2015.
- [22] E. L. Holzman, "Pillbox antenna design for millimeter-wave basestation applications," *IEEE Antennas and Propagation Magazine*, vol. 45, no. 1, pp. 27-37, Mar. 2003.
- [23] K. S. Feng, H. T. Qin, L. Na, Z. X. Liu, and J. Li, "A novel bow-tie feed for dual-layer pillbox antenna," *2014 IEEE International Conference on Signal Processing, Communications and Computing (ICSPCC)*, Guilin, pp. 663-666, 2014.
- [24] L. Chen, D. Liao, X. Guo, J. Zhao, Y. Zhu, and S. Zhuang, "Terahertz time-domain spectroscopy and micro-cavity components for probing samples: A review," *Frontiers of Information Technology & Electronic Engineering*, vol. 20, no. 5, pp. 591-607, May 2019.



**Demiao Chu** received the B.S. degree in Optoelectronic Information Science and Engineering from the Chizhou University, Chizhou, China, in 2019. He is currently working toward the M.S. degree in Optical Engineering at the University of Shanghai for Science and Technology, Shanghai, China. His research interests include millimeterwave and THz imaging technology, especially THz synthetic-aperture radar (SAR) and Cylinder imaging algorithm.



**Yujun Xiong** is currently working toward the M.S. degree in Optical Engineering at the University of Shanghai for Science and Technology, Shanghai, China. His research interests include microwave transmission line and antenna, especially front-end transmission network for MIMO imaging systems and high gain antenna design in terahertz non-destructive testing.



**Ping Li** received the Ph.D. degree from the Northwestern Polytechnical University, Xi'an, China, in 2006. She is currently a Researcher with the University of Shanghai for Science and Technology, Shanghai, China. Her research interests include millimeter-wave and terahertz-wave technology, especially with the Terahertz imaging system.